

# Influence of Fin Shape on Heat Transfer in Coil and Fin type Evaporator

Mateusz PROKOPOWICZ<sup>1</sup>, Andrzej GRZEBIELEC\*<sup>1</sup>

<sup>1</sup> Warsaw University of Technology, Faculty of Power and Aeronautical Engineering,  
Institute of Heat Engineering, Warsaw, Poland

## Abstract

The aim of the study is to investigate the influence of external fins on heat transfer in the evaporator. The scope in which the analysis was performed is to check how the capacity of the exchanger is affected by the change of individual elements of the fin geometry. The introduction describes the current state of knowledge about evaporators. One of the subchapters is entirely devoted to the phenomenon of frosting evaporators, which is unfavourable from the point of view of heat transfer. The subsection also describes how to minimize the occurrence of this phenomenon. The next chapter presents mathematical models of heat transfer coefficients during boiling of inorganic refrigerants in horizontal pipes and during the flow of a bundle of smooth and air-fined pipes. On the basis of correlations and mathematical dependencies contained in this chapter, analyses of the influence of individual factors on heat transfer in the evaporator were performed. The next chapter contains the analysis methodology, it contains drawings of modeled heat exchangers. The penultimate chapter contains the results of the analyses with graphs and descriptions, detailing the most important differences between the individual evaporator geometries. The last chapter is a summary and conclusions about the effect of fins on heat transfer in the evaporator.

**Keywords:** evaporator, fins, lamellar heat exchanger

## 1 Admission

The finning of heat exchangers is intended to increase the heat exchange capacity. The use of fins in the heat exchanger allows to reduce its size while maintaining the same amount of heat exchanged per unit of time.

### 1.1 Evaporator

An evaporator is a type of heat exchanger in which the working medium evaporates. The figures show the basic refrigeration cycle (Figure 1) and the Linde cycle on p-h diagram (Figure 2). The basic, ideal Linde cycle consists of four thermodynamic transformations of the working medium circulating in the installation. These transformations are:

- isentropic compression;
- isobaric condensation;
- isenthalpic expansion;
- isobaric evaporation.

---

\* **Corresponding author:** E-mail address: (andrzej.grzebielec@pw.edu.pl) Andrzej GRZEBIELEC

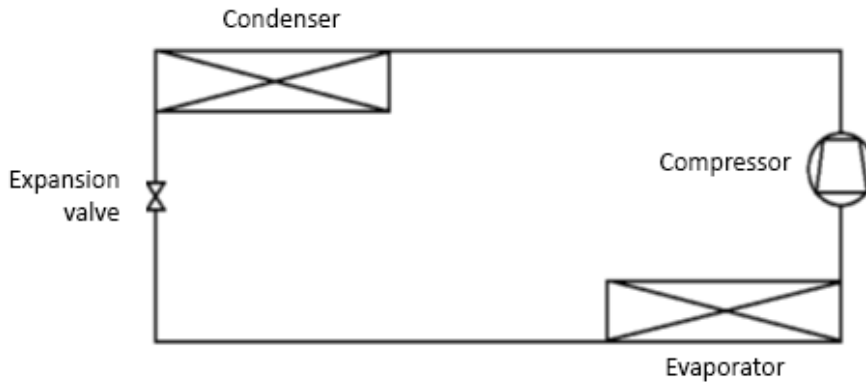


Figure 1. Basic refrigeration system

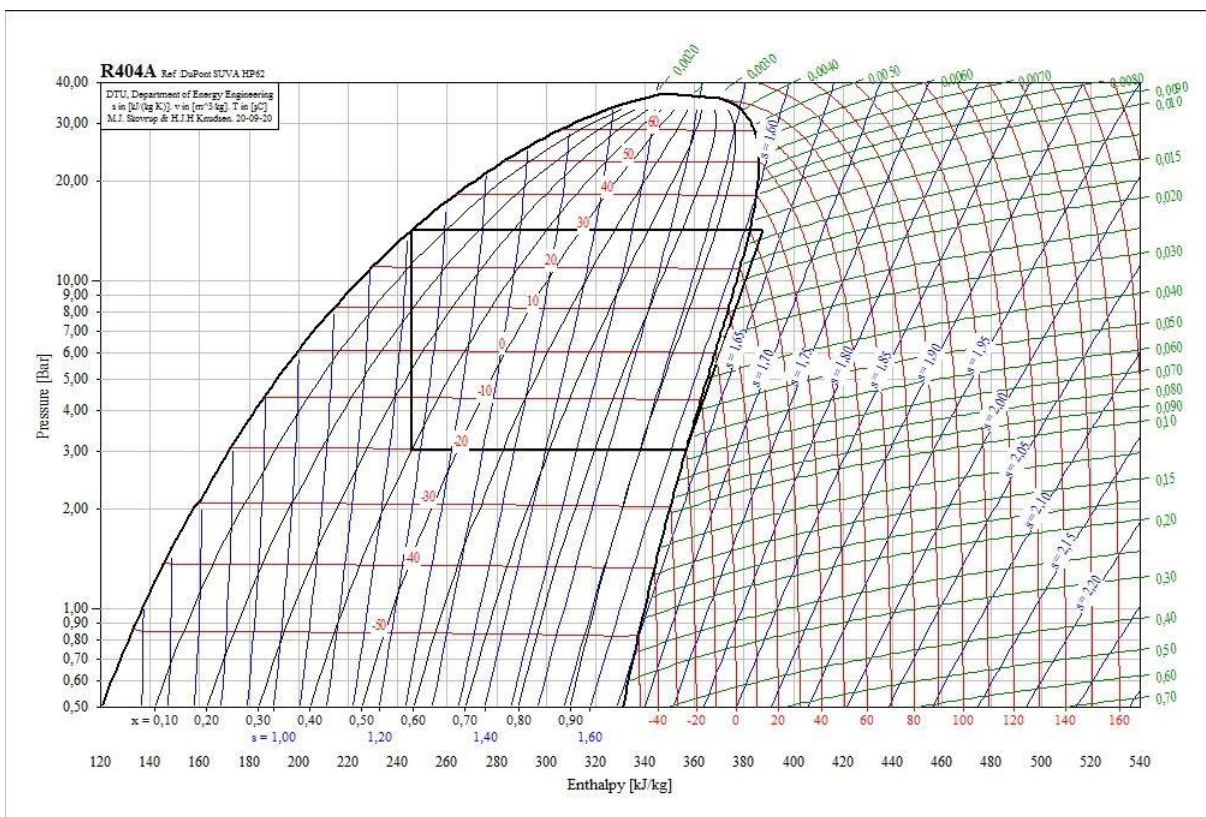


Figure 2. Ideal Linde cycle[18]

This series of transformations allows heat to be transported from a space with a lower temperature to a space with a higher temperature. In the evaporator, isobaric evaporation of the working medium is carried out. The evaporation temperature, and thus the temperature achieved in the cooled space, depends on the working medium and its pressure. Ideally, heat exchange should be carried out with the smallest possible temperature difference between the air and the refrigerant, but the design of the exchangers shows that a temperature difference of 10 – 15 K is necessary to ensure heat exchange.

$$\dot{Q} = A \cdot k \cdot \Delta T \tag{1}$$

Evaporators due to their use can be divided into air coolers designed for cooling chambers and liquid coolers. The cooling process of a given medium can take place directly, by evaporation of the refrigerant, or indirectly, through a secondary fluid, e.g. brine. In air coolers, its cooling can be natural convection or forced by fan operation.



Figure 3. Counterflow heat exchanger

$$\Delta T = \frac{\Delta T_A - \Delta T_B}{\ln\left(\frac{\Delta T_A}{\Delta T_B}\right)} \quad (2)$$

where:

$\Delta T_A$  – temperature difference between streams on the A-side of the exchanger,

$\Delta T_B$  – temperature difference between streams on the B side of the exchanger.

## 1.2 Lamella evaporator

In order to increase the heat exchange surface of the coil evaporators, plates, popularly called lamellas, made of the same or another material are applied to smooth pipes. The shape and arrangement of the sipes must ensure good airflow conditions and easy defrosting. The distances between them range from 3.2 to 12 mm for refrigeration equipment operating at low temperatures, such as freezers. Increasing the spacing between the fins also means a smaller heat transfer surface of the evaporator, contained in 1 linear meter of the finned tube, and therefore a lower cooling capacity. To obtain the same heat flux, a larger and more expensive evaporator must therefore be used. In air conditioning devices, due to higher operating temperatures, and thus the lack of frost, smaller slats are used. The most commonly used pipe and lamella materials are copper, aluminum, stainless steel and stainless steel made of aluminum, sometimes additionally covered with an anti-corrosion plastic layer. The choice of material type in each case depends on the operating conditions of the exchanger and the associated requirements of its corrosion protection. To ensure good heat transfer, it is important to tightly fix the fins on the pipes to minimize contact resistance. Laminated evaporators are currently the most commonly used, primarily in cold rooms, refrigerators, as well as in air conditioning equipment. An example of the design of such an evaporator is shown in Figure 4.



Figure 4. Fin evaporator example [16]

For higher cooling capacities, forced air flow evaporators through the fan are commonly used. A lamellar heat exchanger and axial fans are mounted in a common housing. In addition, a drip tray with a drainage connection designed for drainage of condensate is mounted in the housing. For space cooling applications below +2°C, these coolers are designed to defrost the heat exchanger. Given the mode of operation, these evaporators work as dry. The refrigerant is injected into them from above, through one or more nozzles through a thermostatic expansion valve. In

turn, the fans pump or suck air through the lemel pack in a cross-flow co- or counter-current. Suction design is characterized by the following advantages:

- the air flow through the fins of the evaporator is more even, which provides better conditions for heat exchange taking place in it,
- the outflowing stream of cooled air is more advantageously directed and its width is larger, thanks to which better air circulation and flushing of the cooled space are achieved,
- by distributing the air more evenly within the evaporator, uniform frosting is also achieved, resulting in a shorter defrosting time, which leads to significant energy savings.

In some designs, a variable distance between the fins, e.g. 4.5/9 mm, is used to reduce too fast icing of the exchanger from the air intake side of the cooled space.

## 2 Mathematical models of heat transfer in evaporators

Mathematical models were used to model the evaporator on heat transfer inside the pipe during boiling of the medium flowing through the evaporator, heat conduction through the walls of the tube, and heat transfer at flow, whether lamellar or not, of the pipe bundle.

Heat transfer through the exchanger consists of three stages:

- heat transfer on the inner side,
- heat conduction through the exchanger wall,
- heat transfer on the outer side, including frost.

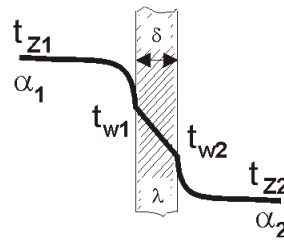


Figure 5. Heat transfer through cylindrical wall [19]

Each of these stages is characterized by a certain thermal resistance. The linear heat transfer resistance on the inner side is given by:

$$r_{conv} = \frac{1}{\alpha_1 \cdot 2\pi d_i} \tag{3}$$

where:

$\alpha_1$  – heat transfer coefficient (inside) [W/(m<sup>2</sup>K)],

$d_i$  – inner diameter [m].

The transfer resistance on the outer side is determined in the same way by assuming the heat transfer coefficient and the outer diameter.

The linear resistance of heat conduction through a cylindrical wall is given by the equation [15]:

$$r_{cond} = \frac{1}{2\pi\lambda} \ln\left(\frac{d_o}{d_i}\right) \tag{4}$$

where:

$d_i$  – inner diameter [m],

$d_o$  – outer diameter [m],

$\lambda$  – wall thermal conductivity coefficient [W/(m·K)].

The linear resistance of heat transfer through the heat exchanger is determined from the formula:

$$r = r_{conv,i} + r_{cond,w} + r_{cond,f} + r_{conv,o} \quad (5)$$

where:

- $r_{conv,i}$  – heat transfer coefficient on the inner side,
- $r_{cond,w}$  – thermal conductivity coefficient through the wall,
- $r_{cond,f}$  – thermal conductivity coefficient through the frost layer,
- $r_{conv,o}$  – heat transfer coefficient on the outside side.

Having a determined linear heat transfer resistance, the power of the exchanger is determined from the formula:

$$\dot{Q} = \frac{\Delta T \cdot l}{r} \quad (6)$$

where:

- $\Delta T$  – temperature difference between boiling fluid and air [K],
- $l$  – pipe length [m].

## 2.1 Heat transfer coefficient at boiling of liquid in horizontal pipes

### 2.1.1 Smooth pipes - Chen model

The heat transfer coefficient from the refrigerant side during boiling can be determined using the Chen formula describing heat transfer at boiling liquids in horizontal pipes [3], determined on the basis of an experiment from 1966, in which the flow of organic and inorganic liquids was studied in the velocity range from 0.1 to 4.5 m/s, temperatures in the range from -40 to 40 °C at a pressure of 1 to 6 bar.

$$\alpha = F \cdot \alpha_{conv} + S \cdot \alpha_b \quad (7)$$

where:

- $\alpha_{conv}$  – heat transfer coefficient during convection of the forced liquid phase,
- $\alpha_b$  – is the heat transfer coefficient for boiling in volume with the same superheat of the liquid,
- $F$  – two-phase flow coefficient, taking into account the increase in the heat transfer coefficient caused by the interaction of the steam phase,
- $S$  – a coefficient compensating for differences between boiling conditions in flow and in volume (decreasing).

The coefficient  $\alpha_{conv}$  is determined from the relationships (' is the value for the liquid, " is the value for the vapor):

$$Nu' = \frac{\alpha_{conv} d_i}{\lambda'} \quad (8)$$

$$Re' = \frac{\dot{M} d_i}{\mu'} \quad (9)$$

$$Nu' = 0.023 \cdot Re'^{0.8} \cdot Pr'^{1/3} \quad (10)$$

The coefficient  $\alpha_b$  describing the boiling in the volume and can be determined from the relationship:

$$\alpha_b = 0.00122 \cdot \frac{\lambda'^{0.79} \cdot c_p'^{0.45} \cdot \rho'^{0.49} \cdot g}{\sigma^{0.5} \cdot \mu'^{0.295} \cdot r^{0.24} \cdot \rho''^{0.24}} \cdot \Delta T^{0.24} \cdot \Delta p^{0.75} \quad (11)$$

$$F = \frac{1}{\chi_{tt}} \quad (12)$$

$$\frac{1}{\chi_{tt}} = \left(\frac{\rho'}{\rho''}\right)^{0.5} \cdot \left(\frac{\mu'}{\mu''}\right)^{0.1} \cdot \left(\frac{x}{1-x}\right)^{0.9} \quad (13)$$

$$S = Re_c \cdot Fr_c^{1.25} \quad (14)$$

$$Fr_c = \frac{m_c^2}{\rho_c^2 \cdot g \cdot d} \quad (15)$$

### 2.1.2 Smooth pipes - Mikielewicz model

Another example of a correlation from which the heat transfer coefficient at boiling of liquids in horizontal pipes can be determined is the Mikielewicz formula [7]:

$$\alpha = \alpha_{conv} \sqrt{R_1^{0.8} + \omega \left(\frac{\alpha_{os}}{\alpha_{conv}}\right)^2} \quad (16)$$

where:

$\alpha_{conv}$  – heat transfer coefficient during single-phase steam flow,  
 $\alpha_{os}$  – co-absorbed heat factor and during boiling in large volume,  
 $R_1$  – correction factors.

The coefficient  $\alpha_{conv}$  can be calculated in the same way like in previous model. The coefficient  $\alpha_{os}$  can be determined from the Kutateladze equation:

$$Nu = 0.44 \cdot Re_o^{0.7} \cdot Pr'^{0.35} \cdot K_p^{0.7} \quad (17)$$

The criteria numbers  $Nu$ ,  $K_p$  and  $Re_o$  are defined as:

$$Nu = \frac{\alpha_{os} \cdot l_o}{\lambda'} \quad (18)$$

$$K_p = \frac{p_n \cdot l_o}{\sigma} \quad (19)$$

$$Re_o = \frac{\dot{q} \cdot l_o \cdot \rho'}{r \cdot \mu' \rho''} \quad (20)$$

In this case, the characteristic linear dimension is the diameter of the detaching gas bubble  $l_o$  with the equation:

$$l_o = \sqrt{\frac{\sigma}{g(\rho' - \rho'')}} \quad (21)$$

The  $R_1$  factor is defined as:

$$R_1 = [f_1 + 2 \cdot (1 - f_1) \cdot x_m](1 - x_m)^{1/3} + x_m^3 \quad (22)$$

$$f_1 = \frac{\mu' c_p' (\lambda')^{1.5}}{\mu'' c_p'' (\lambda'')^{1.5}} \quad (23)$$

The value of the  $\omega$  coefficient can be determined from the equation:

$$\omega = 0.015 \cdot Co^{0.63} \cdot Re'^{1.524} \cdot Bo^{-0.9} \cdot \left(\frac{l_o}{d_i}\right)^{2.791} \cdot K_p^{-1.299} \cdot Pr'^{1/3} \quad (24)$$

Convection number is determined from the formula:

$$Co = R_2 - (1 - f_2) \cdot x_m - f_2 \quad (25)$$

$$R_2 = [f_2 + 2 \cdot (1 - f_2) \cdot x_m](1 - x_m)^{1/3} + x_m^3 \quad (26)$$

$$f_2 = \left(\frac{\mu'}{\mu''}\right)^{0.25} \frac{\rho''}{\rho'} \quad (27)$$

Among these models, the Chen model was chosen for further analysis due to the modeling of boiling during the flow of an inorganic refrigerant at  $-20^\circ\text{C}$  at a pressure of 4 bar in the velocity range from 0.6 to 0.8 m/s.

### 3 Methodology

Two models of heat exchangers were drawn using DesingModeler from ANSYS to perform the analysis:

- a bunch of smooth pipes;
- a bunch of lamellar pipes.

These drawings are illustrative in screenshots below:

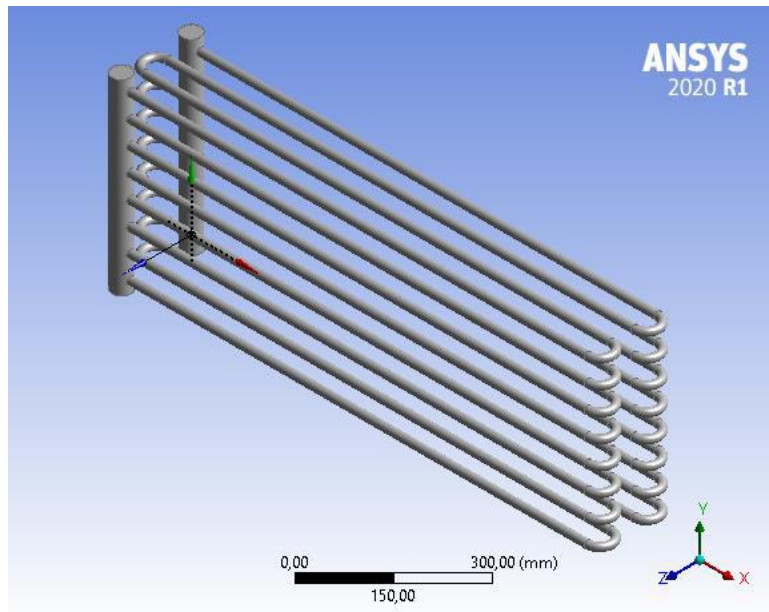


Figure 6. Modeled exchanger - a bunch of smooth pipes



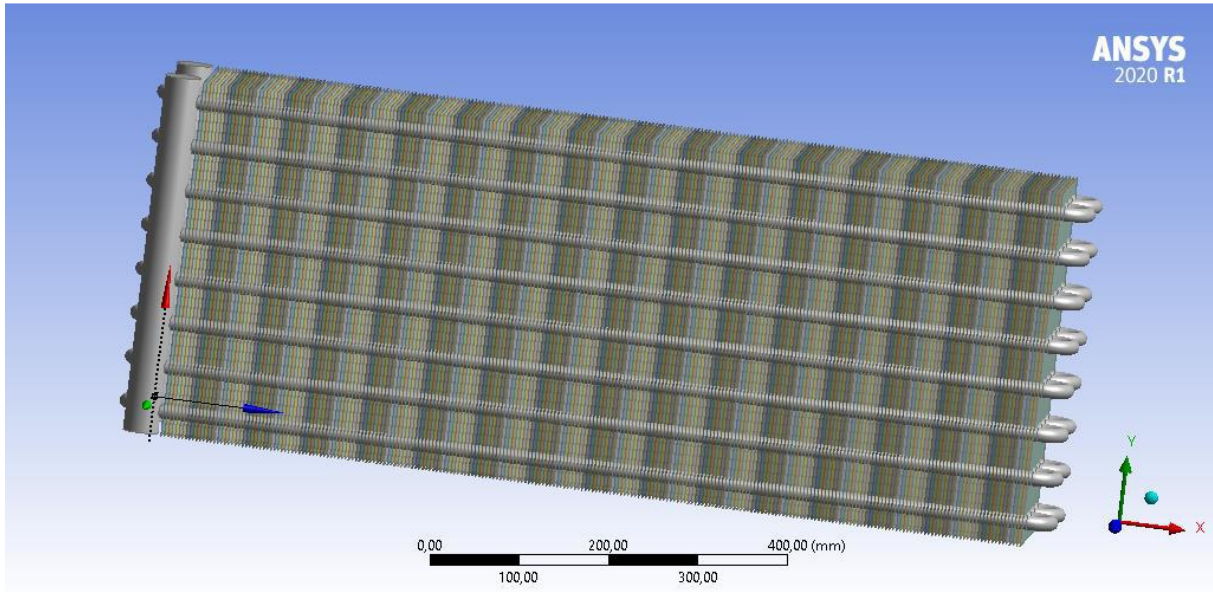


Figure 7. Modeled exchanger - a bunch of lamellar pipes

The geometry of the heat exchanger for which the most parameters are needed, are presented in Table 1.

Table 1. Geometry of heat exchangers

Inner diameter [mm]	14
Outside diameter [mm]	16
Number of pipes per column	8
Number of pipes in a row	4
fin thickness [mm]	0,3
Distance between fins [mm]	4
Length [m]	1
Longitudinal pitch of the pipe system [mm]	50
Transverse pitch of the pipe system [mm]	50

## 4 Results of the analysis

### 4.1 Influence of piping arrangement on heat transfer

Comparison illustrates the differences between the arrangement of pipes in a bundle. The comparison was made for the variable air velocity varying from 1 m/s to 10 m/s, with the other parameters unchanged

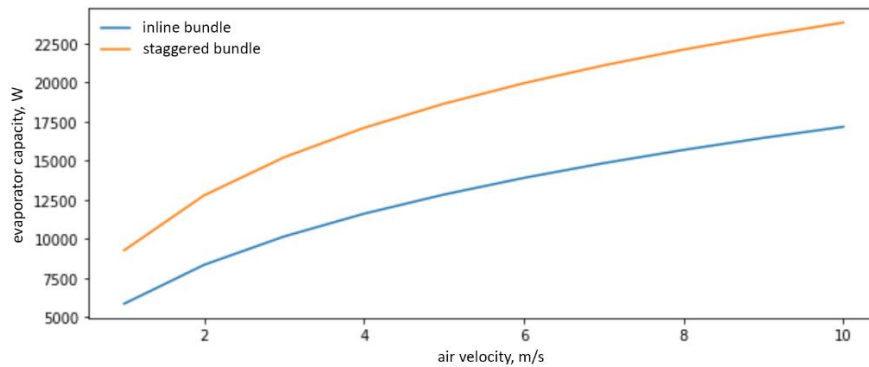


Figure 8. Comparison of lamellar heat exchangers capacity depending on the pipe arrangement for variable air velocity



The results of the analysis presented in the diagram clearly show that significantly more heat is exchanged for a bunch of pipes in a staggered bundle.

### 4.2 Effect of lamella thickness on heat transfer

The next comparison is the effect of the lamella thickness on the heat exchanged by the two lamellar heat exchanger designs. The comparison was carried out for the lamella thickness from 0.1 mm to 1 mm, with the other parameters unchanged. The results of the comparison are presented in the graph.

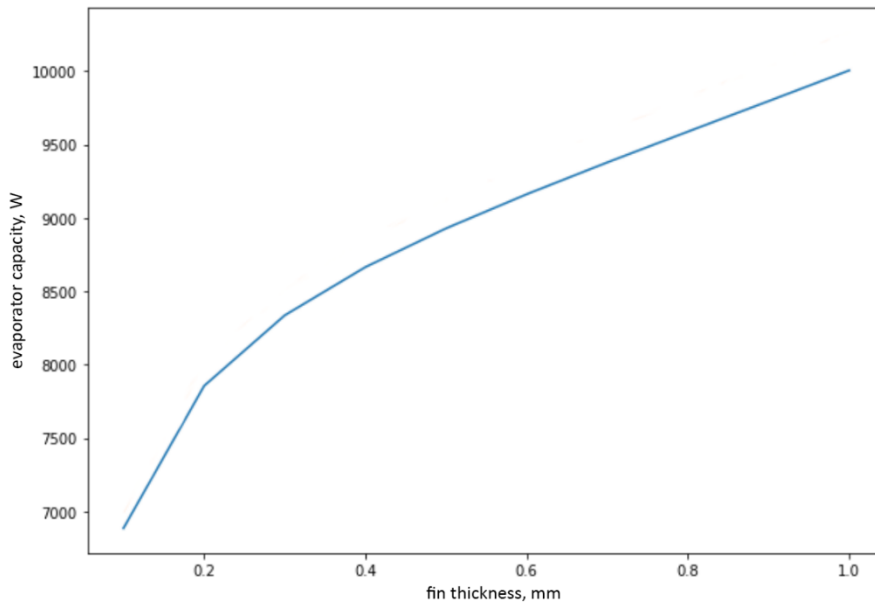


Figure 9. Heat exchanger capacity according to the thickness of the fins

The chart presents the results of the analysis. As the width of the lamella increases, the amount of heat exchanged by the exchanger increases, this is due to the fact that as the thickness of the lamella increases, its efficiency increases.

### 4.3 Influence of distance between fins on heat transfer

Next step it was the comparison due to the distance between the fins. The comparison was made for the distance between the lamellas from 0.5 to 10 mm, with the other parameters unchanged. The comparison is presented in the graph.

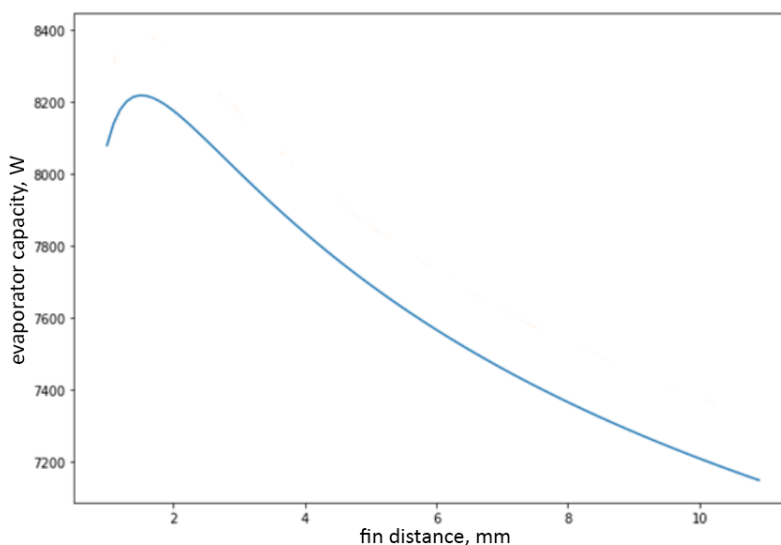


Figure 10. Heat exchanger capacity according to distance between the fins

The analysis shows that the amount of heat exchanged reaches its maximum for a distance between the fins equal to 1.5 mm. This is due to the fact how the air flow through the heat exchanger is shaped. Too high density of lamellas blocks the flow, and a small amount of them significantly reduces the surface of heat transfer from the air side.

**4.4 Influence of frost layer thickness on heat transfer**

The next comparison shows the effect of the thickness of the frost layer on the power of the heat exchanger. It was made for the thickness of frost from 0 to 2 mm, with the other parameters unchanged. The results are shown in the graphs.

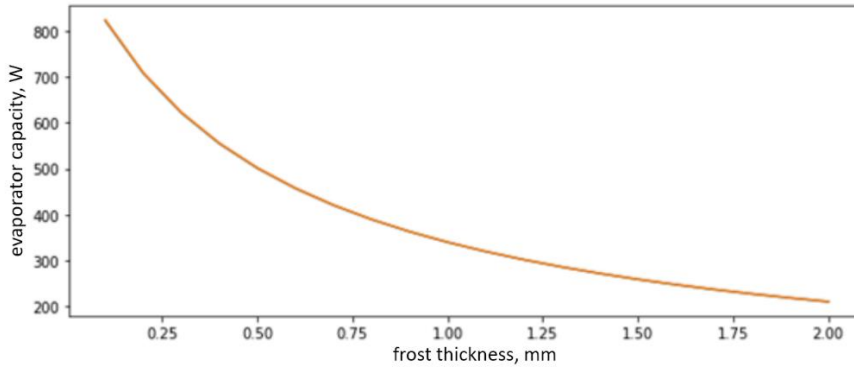


Figure 11. Capacity of non-lamellar heat exchangers according to frost thickness

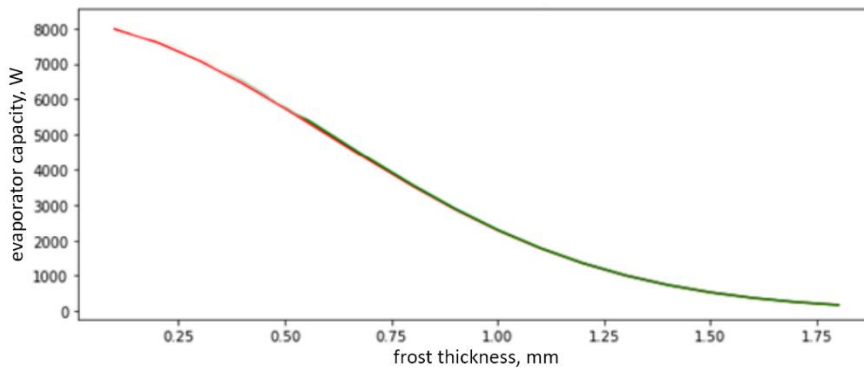


Figure 12. Capacity of lamellar heat exchangers according to frost thickness

The results of the analysis show that frosting has a significant impact on heat transfer in both non-lamellar and lamellar heat exchangers. This is due to the fact that frost with thermal conductivity between  $0.5 - 2 \text{ W / (m}\cdot\text{K)}$  is an insulating layer with high resistance to heat conduction. The capacity drop of the heat exchanger in the case of a lamellar heat exchanger is almost twice as large for the given frost thickness. This is due to the fact that frost mounted on the lamellas not only resists the flow of heat, but also blocks the flow of air, which reduces heat transfer coefficients on the outer side.

**4.5 Influence of frost density on heat transfer**

The last comparison was made for different densities of the 0.5 mm thick frost layer. The density of frost depends on the air velocity and for speeds from 1 to 10 m/s it is from 50 to 430 kg/m<sup>3</sup>, with the other parameters unchanged. The results are shown in the graphs.

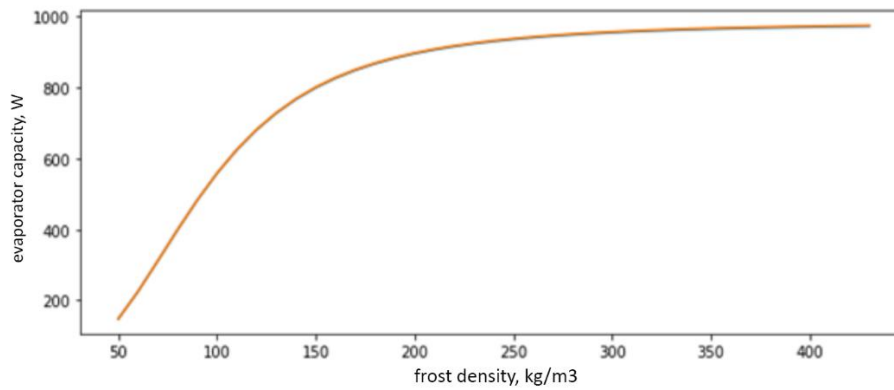


Figure 13. Capacity of non-lamellar heat exchanger depending on frost density

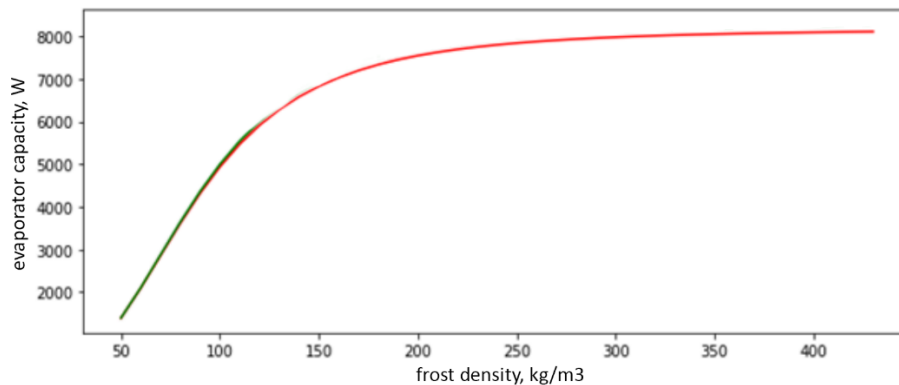


Figure 14. Capacity of lamellar heat exchangers depending on frost density

The graph shows that as the density of frost increases, the amount of heat exchanged by the evaporator increases too. This is because lower density frost is more porous and therefore a better thermal insulator. It can be seen that for the density of frost between 50 and 200 kg / m<sup>3</sup> there is a rather sharp increase in the power of the exchanger. It is worth mentioning that the increase in the power of the exchanger is significantly influenced by the increasing speed of the air in the heat exchanger.

## 5 Conclusions

The finning of the heat exchanger increases the heat exchange surface, thanks to which the density of the heat stream flowing through the heat exchanger increases. In any case, in the comparisons carried out, it can be seen that the influence of external lamellas on heat transfer is significant. The external fins have a great impact, the higher the velocity of the air flowing through the heat exchanger. For an air velocity of 10 m/s for a lamellar heat exchanger, a capacity increase more than 560%. As the thickness of the fins increases, their efficiency increases too, and thus the capacity of the heat exchanger. For the distance between the lamellas, it can be determined a certain distance for which the capacity of the heat exchanger has maximum value. The reason for this is that for small distances between the lamellas, the flow of air is hindered, and as the distance increases, the development of the outer surface decreases. For the analyzed heat exchanger design, this best distance between the fins was 1.5 mm.

Frost has a definitely negative effect on heat exchange in the heat exchanger, for both, lamellar and non-lamellar. For non-lammelar heat exchangers, this impact is significantly smaller, but still significant. The analyses show that even 0.5 mm layer of frost can reduce the heat exchanger capacity by nearly 50%. The density of frost, which is a direct result of the air flow velocity, affects the heat transfer in the heat exchangers. The lower the density of frost, the lower the capacity of the heat exchanger. The largest decrease can be noted for densities between 50 and 200 kg/m<sup>3</sup>. This is due to the fact that less dense frost is more porous and, as a result, it is a better insulator.

## References

1. Bohdal T., Charun H., Czapp M.: *Urządzenia chłodnicze sprężarkowe. Podstawy teoretyczne i obliczenia*,

- Wydawnictwo WNT, Warszawa 2003.
2. Bonca Z., Butrymowicz D., Dambek D., Depta A., Targański W.: *Czynniki chłodnicze i nośniki ciepła. Właściwości cieplne, chemiczne i eksploatacyjne*, IPPU MASTA 1997.
  3. Chen J.C.: *Correlation for boiling heat transfer to saturated fluids in convective flow*, Bookheaven National Library, Nowy Jork 1966, doi:10.1021/i260019a023.
  4. Gogół W.: *Wymiana ciepła. Tablice i wykresy*, Wyd. Politechniki Warszawskiej, Warszawa 1972.
  5. Heide R.: *The surface tension of HFC refrigerants and mixtures*, Elsevier Ltd. Drezno 1997, doi:10.1016/S0140-7007(97)00044-3.
  6. Lixin C., Tingkuan C.: *Flow boiling heat transfer in a vertical spirally internally ribbed tubes*, Heat and Mass Transfer, Eindhoven 2001, doi:10.1007/PL00013294.
  7. Niezgodna-Żelasko B., Zaleski W.: *Chłodnicze i klimatyzacyjne wymienniki ciepła. Obliczenia cieplne*, Wyd. Politechniki Krakowskiej, Kraków 2012.
  8. Ravigururajan T.S.: *General correlations for pressure drop and heat transfer for single-phase turbulent flows in ribbed tubes*, UMI. Iowa 1986, doi:10.31274/rtd-180813-13031.
  9. Seker D., Karatas H., Egrican N.: *Frost formation on fin-and-tube heat exchangers. Part I – Modeling of frost formation on fin-and-tube heat exchangers*, International Journal of Refrigeration. Istanbul 2003, doi:10.1016/j.ijrefrig.2003.12.003.
  10. Szajding A., Telejko T., Rywotycki M., Kuźnia M.: *Wpływ kąta skrzywienia żeber wewnętrznych na proces wymiany ciepła w rurach obustronnie ożebrowanych*, Rynek Energii Nr 5 (102), Warszawa 2012.
  11. Ullrich H.J.: *Technika chłodnicza*, Tom 1. IPPU MASTA 1998.
  12. Ullrich H.J.: *Technika chłodnicza*, Tom 2. IPPU MASTA 1999.
  13. Wen-Tao J., Ding-Cai Z., Ya-Ling H., Wen-Quan T.: *Prediction of fully developed turbulent heat transfer of internal helically ribbed tubes – An extension of Gnielinski equation*, Elsevier Ltd. Xi'an 2011, doi:10.1016/j.ijheatmasstransfer.2011.08.028.
  14. Wiśniewski S.: *Wymiana ciepła*, Wydawnictwo WNT, Warszawa 2013.
  15. Zakrzewski B.: *Odszranianie oziębiaczy powietrza*, WNT, Warszawa 2007.
  16. Product sheet Alfa Laval Fincoil L/J
  17. Katalog z cennikiem, Biwar 2011.
  18. Coolpack v1.5.0.
  19. energia.eco.pl.